Medicinal Chemistry Research (2020) 29:229–242
https://doi.org/10.1007/s00044-019-02477-4

MEDICINAL CHEMISTRY RESEARCH

ORIGINAL RESEARCH

Synthesis, anti-inflammatory evaluation and in silico studies of naphtho[1,2-*e*][1,3]oxazine derivatives as potential non-steroidal anti-inflammatory agents

Leimajam V. Chanu[1] · Khumukcham Nongalleima[2] · Salam P. Singh[2] · Wahengbam K. Chanu[2] · Chingakham B. Singh[2] · Okram M. Singh[1]

Received: 14 August 2019 / Accepted: 9 November 2019 / Published online: 11 December 2019

Abstract

A small molecule library of *trans*-1,3-diaryl-1*H*-naphtho[1,2-*e*][1,3]oxazines **4** is synthesised through multicomponent reactions involving aliphatic amines, aromatic aldehydes and β-naphthol using a heterogeneous catalyst, $SiO_2.HClO_4$, and ethanol as the solvent. The anti-inflammatory activities of the synthesised compounds are evaluated together with in silico studies. 1,3-Bis(4-chlorophenyl)-2-ethyl-2,3-dihydro-1*H*-naphtho[1,2-*e*][1,3]oxazine (**4h**) shows the best activity with $IC_{50} = 4.807$ μg/mL in the heat-induced haemolysis, while 1,3-Bis(5-bromothiophen-2-yl)-2-ethyl-2,3-dihydro-1*H*-naphtho [1,2-*e*][1,3]oxazine (**4c**) shows significantly high anti-inflammatory activity ($IC_{50} = 5.5$ μg/mL) in comparison with standard drugs, such as sodium diclofenac. In addition, molecular docking simulation study confirms the in-depth molecular interaction of the two lead compounds, **4c** and **4h** with better binding affinities and docking scores at the active site of the COX-2 enzyme compared with diclofenac.

Highlights

- $SiO_2.HClO_4$ as a heterogeneous catalyst in the synthesis of naphtho[1,2-*e*][1,3]oxazine.
- The anti-inflammatory activities of the synthesised compounds were also analysed along with the in silico studies.
- The importance of naphtho[1,2-*e*][1,3]oxazine are highlighted.
- The catalyst is easily accessible and reusable.

Keywords Oxazine · Amines · Aldehydes · *β*-naphthol · Heterogeneous catalyst · Anti-inflammatory

Introduction

Inflammation is the reaction process of living tissues to stimuli induced by inflammatory agents, such as physical injuries, heat, microbial infections, and noxious chemical irritants, where the response of cells toward inflammation will lead to appear certain pathological indicators, such as redness, heat, swelling, and pain, sometimes with impaired physiological functions (Ruedi et al. 2008; Artis and Spits 2015). The occurrence of inflammation can be associated with a number of disorders and is prominently related to painful conditions resulting from tissue injury, cell death, cancer, and ischaemia (Lucas et al. 2006; Rock et al. 2011; Waisman et al. 2015).

Important inflammatory mediators, such as prostaglandins, prostacyclin, and thromboxane, are produced through the prostanoid biosynthetic pathway from

These authors contributed equally: Leimajam V. Chanu, Khumukcham Nongalleima

Supplementary information The online version of this article (https://doi.org/10.1007/s00044-019-02477-4) contains supplementary material, which is available to authorised users.

✉ Okram M. Singh
ok_mukherjee@yahoo.co.in

[1] Department of Chemistry, Manipur University, Imphal, 795003 Manipur, India

[2] Institute of Bioresource and Sustainable Development, Imphal, 795001 Manipur, India

arachidonic acid using cyclooxygenase (COX) as a key enzyme (Kurumbail et al. 1996). The COX enzyme exists in two different forms, cyclooxygenase 1 (COX-1) and cyclooxygenase 2 (COX-2). COX-2 is associated with inflammation and the resulting pain. Thus, to inhibit the activity of the COX-2 enzyme, many non-steroidal anti-inflammatory drugs (NSAIDs) have been developed (Hawkey 1999). However, the use of such drugs results in many side effects such as, ulcerogenic, cardiovascular effects, etc. (Lanas and Chan 2017; Trelle et al. 2011). In view of occurrence of these adverse side effects, we have been interested in the development of novel non-steroidal anti-inflammatory compounds with minimum side effects.

1,3-Oxazine and its derivatives constitute an important class of heterocyclic compounds, which occupy a unique place in medicinal chemistry because of their wide spectrum of biological properties, such as antimicrobial (Mathew et al. 2010), antitubercular (Mathew et al. 2010), anti-HIV (Cocuzza et al. 2001), antimalarial (Ren et al. 2001), anticoagulant (Riveiro et al. 2010), anticonvulsant (Kurz 2005), antitubular (Zhang et al. 2003), antithrombotic (Hsieh et al. 2005), and antitumour activities (Fig. 1a–c) (Benameur et al. 1996). They also play an important role as a monomer in the polymer industry (Wang and Ishida 2000). Further, they act as important precursors in various organic transformations (Lee et al. 2012; Kajjout et al. 2013) and in the total synthesis of natural products (Fig. 2a, b) (Ji-Yeon et al. 2011; Park et al. 2015; Jin et al. 2014). However, only a few relevant studies on the anti-inflammatory activity of 1,3-oxazine derivatives have been reported (Yan-Fei et al. 2016; Puwen et al. 2002). Moreover, the potential of naphtho[1,2-*e*][1,3]oxazine derivatives against the inflammatory enzyme COX-2 has remained unexplored.

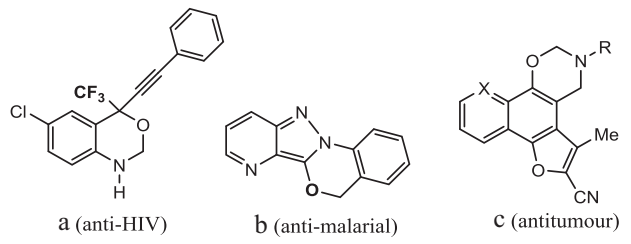

Fig. 1 1,3-Oxazines-fused bioactive heterocycles

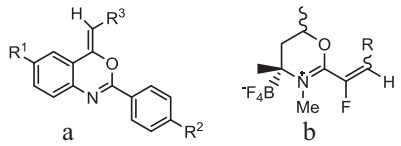

Fig. 2 1,3-Oxazines as precursors for the synthesis of natural products for their preparation

One of the factors for the lack of reports on the anti-inflammatory activity of naphtho[1,2-*e*][1,3]oxazines may be due to a few synthetic methods available in the literature (Harish et al. 2012; Istvan et al. 2004; Daqing et al. 2010; Maria et al. 2016). Thus, we undertook the challenge of developing new and convenient methods for synthesising naphtho[1,2-*e*][1,3]oxazines and studying their potential as anti-inflammatory agents. Our research group has been interested in the synthesis of bioactive heterocycles involving cascade/domino reactions, either through multi-component reactions (MRCs) or one-pot, sequential convergent reactions (Okram et al. 2008; Prasanta et al. 2013; Thokchom et al. 2018; Leimajam et al. 2018). Thus, we report herewith an efficient and diastereoselective synthesis of a series of *trans*-1,3-diaryl-1*H*-naphtho[1,2-*e*][1,3]oxazines **4** based on an MCR involving aliphatic amines, aromatic aldehydes, and β-naphthol using a heterogeneous catalyst, $SiO_2.HClO_4$, with ethanol as the solvent. The potential activity of these compounds against inflammation with supporting information from in silico studies is presented in this report as a short commentary.

Experimental

Chemistry

Materials and reagent

All reagents and solvents were purchased from commercial sources, such as Merck and Aldrich, and were used as received. ^{1}H NMR (400 MHz) and ^{13}C NMR (100 MHz) spectra were recorded on FT-NMR spectrometer using $CDCl_3$ and d_6-DMSO. Chemical shifts δ are measured in parts per million (ppm) and are relative to tetramethylsilane as the internal reference. Data are reported as follows: chemical shift, multiplicity (s = singlet, d = doublet, t = triplet, m = multiplet, br = broad) and coupling constants (*J*) in Hertz. The FT-IR spectra were recorded on a Perkin-Elmer FT-IR spectrometer (KBr). Melting points were determined on a 'Veego' capillary melting point apparatus and are uncorrected. Silica gel 60–120 was used for column separations. Chemical yields refer to pure isolated substances. Mass, COSY, and NOESY spectra were also taken in a Bruker SFO1 400 MHz.

Preparation of the catalyst, $SiO_2.HClO_4$

We started with the preparation of the heterogeneous catalyst, $SiO_2.HClO_4$. In this procedure, to a suspension of SiO_2 (230–400 mesh, 11.6 g) in diethylether (40 mL), 70% aqueous perchloric acid (1.3 g, 9.4 mmol) was added. Then, the mixture was kept for overnight and the residue was heated

at 100 °C for 72 h. The residue was washed several times with diethyl ether.

Preparation of 1,3-oxazine, 4a

A mixture of benzaldehyde (2 mmol), ethylamine (1 mmol), and β-naphthol (1 mmol) was refluxed in ethanol using 4 mol% $SiO_2.HClO_4$. The reaction was monitored by thin layer chromatography. After refluxing for 18 h, ethanol was evaporated using rotary vacuum evaporator. Water (50 mL) was added to the residue followed by ethyl acetate (50 mL). The ethyl acetate extract was treated with anhydrous sodium acetate and the product was isolated from column chromatography.

Characterisation data of compounds 4a–4n

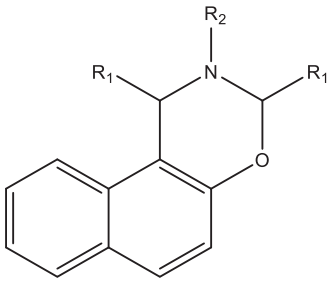

2-Ethyl-1,3-diphenyl-2,3-dihydro-1H-naphtho[1,2-*e*][1,3] oxazine, 4a White crystal, melting point 143–145 °C. ^{1}HNMR (400 MHz, $CDCl_3$, δ ppm): 1.00 (3H, t, $J = 8$), 1.4 (2H, q, $J = 9.6$), 5.3 (1H, s), 5.7 (1H, s), 7–7.16 (10H, m), 7.23–7.25 (2H, d, $J = 5.6$), 7.37–7.35 (2H, d, $J = 9.6$), 7.58–7.56 (1H, d, $J = 9.6$), 7.62–7.60 (1H, d, $J = 8.4$); ^{13}CNMR (100 MHz, $CDCl_3$, δ ppm): 14.42, 21, 39, 58, 87, 112, 119, 124, 126, 127, 129, 130, 134, 136, 138, 139, 141, 153; IR (KBr) (ν max, cm^{-1}): 3062, 2946, 2848, 1601, 1507, 1452, 1392, 1333, 1233, 1125, 945, 813, 700. ESI-MS *m/z*: 366.18, calcd. for $C_{26}H_{23}NO$ $(M + H)^+$: 365.18; CHN analysis (%): cal. C, 82.95; H, 8.41; N, 4.03; found C, 82.79; H, 8.44; N, 4.01.

2-Ethyl-1,3-bis(4-methoxyphenyl)-2,3-dihydro-1H-naphtho [1,2-*e*][1,3]oxazine, 4b Yellow crystal, melting point 159–161 °C. ^{1}HNMR (400 MHz, $CDCl_3$, δ ppm): 1.00 (3H, t, $J = 8$), 1.4 (2H, q, $J = 9.6$), 3.7 (3H, s), 3.8 (3H, s), 5.4 (1H, s), 5.7 (1H, s), 7–7.16 (8H, m), 7.23–7.25 (2H, d, $J = 5.6$), 7.37–7.35 (2H, d, $J = 9.6$), 7.58–7.56 (1H, d, $J = 9.6$), 7.62–7.60 (1H, d, $J = 8.4$); ^{13}CNMR (100 MHz, $CDCl_3$, δ ppm): 14.42, 21, 39.5, 59.2, 87, 113, 118, 122, 126, 127, 129, 130, 133, 136, 137, 138, 140, 152; IR (KBr) (ν max, cm^{-1}): 3062, 2946, 2848, 1601, 1507, 1452, 1392, 1333, 1233, 1125, 945, 813, 700. ESI-MS *m/z*: 426.20, calcd. for $C_{28}H_{27}NO_3$ $(M + H)^+$: 425.53; CHN analysis (%): cal. C, 79.03; H, 6.40; N, 3.29; found C, 78.01; H, 6.47; N, 3.26.

1,3-Bis(5-bromothiophen-2-yl)-2-ethyl-2,3-dihydro-1H-naphtho[1,2-*e*][1,3]oxazine, 4c Brown crystal, melting point 137–138 °C. ^{1}H NMR (400 MHz, $CDCl_3$, δ ppm): 1.3 (3H, t, $J = 4$), 2.4 (2H, q, $J = 8$), 5.6 (1H, s), 6.1 (1H, s), 6.63–6.64 (1H, d, $J = 4$), 6.77–6.79 (1H, d, $J = 8$), 7.01–7.0 (1H, d, $J = 8$), 7.21–7.69 (2H, m), 7.71–7.81 (3H, m). ^{13}C NMR (100 MHz, $CDCl_3$, δ ppm): 18.5, 43.9, 57.9, 110, 119, 123.3, 125.4, 126.5, 127.6, 127.8, 128, 131.8, 135.8, 138.8, 142.9, 147.5. IR (KBr) (ν max, cm^{-1}): 3789, 2927, 1899, 1379, 1299, 1195, 1026, 990, 650. ESI-MS *m/z*: 380.20, calcd. for $C_{22}H_{17}Br_2NOS_2$ $(M + H)^+$: 532.19; CHN analysis (%): cal. C, 71.90; H, 4.87; N, 3.22; found; C, 69.97; H, 4.67; N, 3.17.

2-Ethyl-1,3-di-p-tolyl-2,3-dihydro-1H-naphtho[1,2-*e*][1,3] oxazine, 4d White semi crystal, melting point 137–139 °C. ^{1}H NMR (400 MHz, $CDCl_3$, δ ppm): 1.14–1.16 (3H, t, $J = 8$), 2.3 (6H, s), 2.6–2.7 (2H, q, 4), 5.5 (1H, s), 5.7 (1H, s), 7.01–7.16 (8H, m), 7.08–7.09 (1H, d, $J = 7$), 7.78–7.76 (2H, d, $J = 8$), 7.4–7.3 (2H, d, $J = 7$), 7.7–7.8 (1H, d, $J = 8$). ^{13}C NMR (100 MHz, $CDCl_3$, δ ppm): 14.5, 21.2, 21.3, 39.5, 58.0, 86.0, 112.8, 119.1, 123.2, 123.3, 126.4, 128.6, 129.1, 129.5, 135.5, 136.7, 137.3, 140.5, 153.0; IR (KBr) (ν max, cm^{-1}): 3059, 2943, 2849, 1600, 1505, 1456, 1392, 1323, 1231, 1125, 945, 812, 704. ESI-MS *m/z*: 394.21, calcd. for $C_{28}H_{27}NO$ $(M + H)^+$: 393.21; CHN analysis (%): cal. C, 85.46; H, 6.92; N, 3.56; found C, 85.41; H, 6.89; N, 3.45.

2-Ethyl-1,3-bis(4-fluorophenyl)-2,3-dihydro-1H-naphtho [1,2-*e*][1,3]oxazine, 4e White crystalline, melting point 119–121 °C. 1H NMR (400 MHz, $CDCl_3$, δ ppm) 1.01 (3H, t, $J = 8$), 1.3 (2H, q, $J = 9.6$), 5.4 (1H, s), 5.6 (1H, s), 7.01–7.16 (8H, m), 7.22, 7.26 (2H, d, $J = 5.6$), 7.38–7.34 (2H, d, $J = 9.6$), 7.59–7.55 (1H, d, $J = 9.6$), 7.63–7.59 (1H, d, $J = 8.4$); ^{13}CNMR (100 MHz, $CDCl_3$, δ ppm): 14.4, 21, 39.1, 58, 86, 113, 115, 124, 126, 127.2, 129, 131, 133.1, 136, 137.5, 139, 141, 153; 162 (d, $J_{C\text{-}F} = 43.2$ Hz), 163 (d, $J_{C\text{-}F} = 43.3$ Hz); IR (KBr) (ν max, cm^{-1}): 3062, 2946, 2848, 1601, 1507, 1452, 1392, 1333, 1233, 1125, 945, 813, 700. ESI-MS *m/z*: 399, calcd. for $C_{26}H_{19}F_2NO$: $(M + H)^+$: 402.12; CHN analysis (%): cal. C, 77.79; H, 5.27; F, 9.46; N, 3.49; found; C, 77.75; H, 5.23; N, 3.51.

2-Ethyl-1,3-di-o-tolyl-2,3-dihydro-1H-naphtho[1,2-*e*][1,3] oxazine, 4f White crystal, melting point 133–135 °C. 1H NMR (400 MHz, $CDCl_3$, δ ppm): 1.14–1.17 (3H, t, $J = 8$), 2.3 (6H, s), 2.6–2.7 (2H, q, 4), 5.6 (1H, s), 5.7 (1H, s), 7.08–7.45 (10H, m), 7.78–7.76 (2H, d, $J = 8$), 7.88–7.87

(2H, d, $J = 4$). ^{13}C NMR (100 MHz, $CDCl_3$, δ ppm) 14.5, 21.2, 21.3, 39.5, 58.0, 86.0, 112.8, 119.1, 123.2, 123.3, 126.4, 128.6, 129.1, 129.5, 135.5, 136.7, 137.3, 140.5, 153.0. IR (KBr) (ν max, cm^{-1}): 3058, 2943, 2849, 1601, 1505, 1456, 1392, 1323, 1231, 1125, 945, 810, 701. ESI-MS *m/z*: 394.21, calcd. for $C_{28}H_{27}NO$ $(M + H)^+$: 393.21; CHN analysis (%): cal. C, 85.46; H, 6.92; N, 3.56; found; C, 84.89; H, 6.78; N, 3.42.

2-Ethyl-1,3-di(thiophen-2-yl)-2,3-dihydro-1H-naphtho[1,2-*e*][1,3] oxazine, 4g Yellow crystal solid. Melting point 125–126 °C. ^{1}H NMR (400 MHz, $CDCl_3$, δ ppm): 1.3 (3H, t, $J = 4$), 2.4 (2H, q, $J = 8$), 5.6 (1H, s), 6.1 (1H, s), 6.61–6.62 (1H, d, $J = 4$), 6.77–6.79 (1H, d, $J = 8$), 7.02–7.04 (1H, d, $J = 8$), 7.21–7.69 (6H, m), 7.71–7.81 (3H, m); ^{13}C NMR (100 MHz, $CDCl_3$, δ ppm): 18.5, 43.9, 57.9, 110, 119, 123, 125, 126.5, 127.2, 127.6, 128.2, 131.8, 135.8, 138.8, 142.9, 147.5; IR (KBr) (ν max, cm−1): 3788, 2924, 1897, 1375, 1289, 1196, 1029, 996, 650. ESI-MS *m/z*: 406.13, calcd. for $C_{24}H_{23}NOS_2$ $(M + H)^+$: 405.12; CHN analysis (%): cal. C, 69.99; H, 5.07; N, 3.71; found; C, 68.91; H, 5.15; N, 4.10.

1,3-Bis(4-chlorophenyl)-2-ethyl-2,3-dihydro-1H-naphtho[1,2-*e*][1,3]oxazine, 4h White crystal, melting point 117–118 °C. ^{1}HNMR (400 MHz, $CDCl_3$, δ ppm): 1.00 (3H, t, $J = 8$), 1.4 (2H, q, $J = 9.6$), 5.3 (1H, s), 5.7 (1H, s), 7–7.16 (8H, m), 7.23–7.25 (2H, d, $J = 5.6$), 7.37–7.35 (2H, d, $J = 9.6$), 7.58–7.56 (1H, d, $J = 9.6$), 7.62–7.60 (1H, d, $J = 8.4$); ^{13}CNMR (100 MHz, $CDCl_3$, δ ppm): 14.42, 21, 39, 58, 87, 112, 119, 124, 126, 127, 129, 130, 134, 136, 138, 139, 141, 153; IR (KBr) (ν max, cm^{-1}): 3062, 2946, 2848, 1601, 1507, 1452, 1392, 1333, 1233, 1125, 945, 813, 700. ESI-MS *m/z*: 435.10, calcd. for $C_{26}H_{21}Cl2NO$ $(M + H)^+$: 434.36; CHN analysis (%): cal. C, 49.36; H, 3.20; N, 2.62; found C, 50.01; H, 2.98; N, 2.69.

2-Ethyl-1,3-bis(4-nitrophenyl)-2,3-dihydro-1H-naphtho[1,2-*e*][1,3]oxazine, 4i White powder, melting point 153–155 °C. ^{1}H NMR (400 MHz, $CDCl_3$, δ ppm): 1.1 (3H, t, $J = 8$), 1.4 (2H, q, $J = 9.6$), 5.3 (1H, s), 5.7 (1H, s), 7–7.16 (8H, m), 7.23–7.25, (2H, d, $J = 5.6$), 7.37–7.35 (2H, d, $J = 9.6$), 7.58–7.56 (1H, d, $J = 9.6$), 7.62–7.60 (1H, d, $J = 8.4$); ^{13}C NMR (100 MHz, $CDCl_3$, δ ppm): 14.5, 21, 39, 57, 87, 112, 117, 122, 124, 126, 128, 130, 132, 134, 137, 139, 141, 153; IR (KBr) (ν max, cm^{-1}): 3052, 2936, 2841, 1601, 1507, 1452, 1392, 1333, 1233, 1125, 945, 813, 699. ESI-MS *m/z*: 456.15, calcd. for $C_{26}H_{21}N_3O_5$ $(M + H)^+$: 455.15; CHN analysis (%): cal. C, 68.56; H, 4.65; N, 9.23; found; C, 67.67; H, 4.78; N, 8.98.

1,3-Diphenyl-2-propyl-2,3-dihydro-1H-naphtho[1,2-*e*][1, 3] oxazine, 4j White-brown amorphous solid, melting point 135–137 °C. ^{1}H NMR (400 MHz, $CDCl_3$, δ ppm): 0.89 (3H, t, $J = 8$), 1.6 (2H, t, $J = 9.6$), 2.5 (2H, m, $J = 8$), 5.3 (1H, s), 5.7 (1H, s), 7–7.16 (3H, m), 7.18–7.10 (3H, m), 7.23–7.25 (2H, d, $J = 5.6$), 7.37–7.35 (2H, d, $J = 9.6$), 7.58–7.56 (1H, d, $J = 9.6$), 7.57–7.60 (4H, m), 7.62–7.60 (1H, d, $J = 8.4$); ^{13}C NMR(100 MHz, $CDCl_3$, δ ppm): 14.42, 21, 39, 58, 87, 112, 119, 122, 123, 124, 125, 126, 127, 128, 129, 138, 139, 141, 153; IR (KBr) (ν max, cm^{-1}): 3062, 2946, 2848, 1601, 1507, 1452, 1392, 1333, 1233, 1125, 945, 813, 700. ESI-MS *m/z*: 380.20, calcd. for $C_{27}H_{25}NO$ $(M + H)^+$: 379.19; CHN analysis (%): cal. C, 84.25; H, 5.72; N, 4.68; found; C, 83.98; H, 5.56; N, 4.53.

1,3-Bis(4-chlorophenyl)-2-propyl-2,3-dihydro-1H-naphtho[1,2-*e*][1,3]oxazine, 4k White crystal solid, melting point 162–164 °C. ^{1}H NMR (400 MHz, $CDCl_3$, δ ppm): 0.89 (3H, t, $J = 8$), 2.5 (2H, t, $J = 9.4$), 2.5 (2H, t, $J = 8$), 5.4 (1H, s), 5.7 (1H, s), 7–7.16 (4H, m), 7.23–7.25 (2H, d, $J = 5.6$), 7.26–7.28 (2H, d, 5.7), 7.30–7.32 (2H,d, $J = 8$), 7.34–7.36 (2H, d, $J = 8$), 7.58–7.56 (1H, d, $J = 9.6$), 7.62–7.60 (1H, d, $J = 8.4$); ^{13}C NMR(100 MHz, $CDCl_3$, δ ppm): 14, 21, 39, 58, 87, 112, 119, 122, 123, 124, 125, 126, 127, 128, 129, 138, 140, 141, 153; IR (KBr) (ν max, cm^{-1}): 3061, 2916, 2848, 1601, 1504, 1451, 1391, 1332, 1232, 1125, 945, 813, 704. ESI-MS *m/z*: 448.12, calcd. for $C_{27}H_{23}Cl_2NO$ $(M + H)^+$: 447.12; CHN analysis (%): cal. C, 72.33; H, 5.17; N, 3.12; found; C, 71.89; H, 4.97; N, 3.34.

1,3-Bis(4-nitrophenyl)-2-propyl-2,3-dihydro-1H-naphtho [1,2-*e*][1,3]oxazine, 4l White solid, melting point 139–140 °C. ^{1}H NMR (400 MHz, $CDCl_3$, δ ppm): 0.89 (3H, t, $J = 8$), 2.5 (2H, t, $J = 9.4$), 2.5 (2H, t, $J = 8$), 5.4 (1H, s), 5.7 (1H, s), 7–7.16 (4H, m), 7.23–7.25 (2H, d, $J = 5.6$), 7.26–7.28 (2H, d, 5.7), 7.30–7.32 (2H, d, $J = 8$), 7.34–7.36 (2H, d, $J = 8$), 7.58–7.56 (1H, d, $J = 9.5$), 7.62–7.60 (1H, d, $J = 8.3$); ^{13}C NMR (100 MHz, $CDCl_3$, δ ppm): 14, 21, 39, 58, 87, 112, 119, 122, 123, 124,125, 126, 127, 128, 129, 138, 140, 141, 153; IR (KBr) (ν max, cm^{-1}): 3061, 2915, 2848, 1601, 1504, 1451, 1391, 1332, 1232, 1225, 945, 814, 705. ESI-MS *m/z*: 470.17, calcd. for $C_{27}H_{23}N_3O_5$ $(M + H)^+$: 469.16; CHN analysis (%): cal. C, 69.07; H, 4.94; N, 8.95; found; C, 67.98; H, 4.55; N, 7.98.

1,3-Bis(4-methoxyphenyl)-2-propyl-2,3-dihydro-1H-naphtho[1,2-*e*][1,3]oxazine,4m White crystalline solid, melting point 152–153 °C. 0.89 (3H, t, $J = 8$), 2.5 (2H, t, $J = 9.4$), 2.5 (2H, t, $J = 8$), 3.8 (6H, s), 5.4 (1H, s), 5.7 (1H, s), 7–7.16 (4H, m), 7.23–7.25 (2H, d, $J = 5.6$), 7.37–7.35 (2H, d, $J = 9.6$), 7.22–7.24 (2H, d, $J = 5.5$), 7.36–7.34 (2H, d, $J = 9.4$), 7.58–7.56 (1H, d, $J = 9.6$), 7.62–7.60 (1H, d, $J = 8.4$); ^{13}CNMR (100 MHz, $CDCl_3$, δ ppm): 10.42, 21.55, 44.2, 58.2, 60.6, 78.95, 85.49, 113.01, 120.05, 123.29, 126.40, 126.55, 127.13, 127.68, 128.05, 128.05, 128.13,

128.13, 128.60, 128.60, 129.08, 129.52, 129.52, 133.21, 138.25, 143.30, 152.90, 159.80; IR (KBr) (ν max, cm^{-1}): 3052, 2945, 2847, 1621, 1506, 1451, 1394, 1334, 1233, 1125, 945, 813, 708. ESI-MS *m/z*: 440.22, calcd. for $C_{29}H_{29}NO_3$ $(M + H)^+$: 439.21; CHN analysis (%): cal. C, 79.24; H, 6.65; N, 3.19; found; C, 78.99; H, 6.53; N, 2.96.

1,3-Bis(4-fluorophenyl)-2-propyl-2,3-dihydro-1H-naphtho [1,2-*e*][1,3]oxazine, 4n White crystal solid, melting point 140–141 °C. ^{1}H NMR (400 MHz, $CDCl_3$, δ ppm): 0.89 (3H, t, $J = 8$), 2.5 (2H, t, $J = 9.4$), 2.5 (2H, t, $J = 8$), 5.4 (1H, s), 5.7 (1H, s), 7–7.16 (4H, m), 7.23–7.25 (2H, d, $J = 5.6$), 7.37–7.35 (2H, d, $J = 9.6$), 7.22–7.24 (2H, d, $J = 5.5$), 7.36–7.34 (2H, d, $J = 9.4$), 7.58–7.56 (1H, d, $J = 9.6$), 7.62–7.60 (1H, d, $J = 8.4$); ^{13}C NMR (100 MHz, $CDCl_3$, δ ppm): 14.32, 39.52, 58.27, 84.95, 111.49, 119.02, 123.05, 123.29, 126.40, 126.55, 126.13, 127.68, 128.05, 128.05, 128.13, 128.12, 128.64, 128.60, 129.07, 129.52, 129.52, 133.21, 138.25, 143.30, 152.90, 162 (d, $J_{C\text{-}F} = 43.4$ Hz), 163 (d, $J_{C\text{-}F} = 43.5$ Hz); IR (KBr) (ν max, cm^{-1}): 3061, 2915, 2848, 1601, 1504, 1451, 1391, 1332, 1232, 1225, 945, 814, 705. ESI-MS *m/z*: 416.18, calcd. for $C_{27}H_{23}F_2NO$ $(M + H)^+$: 415.17; CHN analysis (%): cal. C, 78.05; H, 5.58; N, 3.37; found; C, 77.89; H, 5.32; N, 3.76.

Pharmacological screening

Erythrocyte suspension preparation

Fresh whole blood (5 mL) was collected from healthy volunteers into heparinized tubes. It was then centrifuged at 3000 × rpm for 10 min. The volume of normal saline equivalent to that of the supernatant was used to dissolve the red blood pellets. The volume of the dissolved red blood pellets obtained was measured and reconstituted as a 40% v/v suspension with isotonic buffer solution (10 mM sodium phosphate buffer, pH 7.4). The buffer solution contained 0.2 g of NaH_2PO_4, 1.15 g of Na_2HPO_4 and 9 g of NaCl in 1 L of distilled water. The reconstituted red blood cells (RBCs) (resuspended supernatant) were used as such.

Heat induced haemolysis

Samples of the extract used were dissolved in isotonic phosphate buffer solution. A set of five centrifuge tubes containing, respectively, 5 mL graded doses of the extracts (100, 200, 400, 600, and 800 µg/mL) were arranged in quadruplicate sets (four sets per dose). Two sets of control tubes contained 5 mL of the vehicle and 5 mL of 200 µg/mL of diclofenac, respectively. Human red blood cells, HRBC, suspension (0.1 mL) was added to each of the tubes and mixed gently. A pair of the tubes was incubated at 54 °C for 20 min in a regulated water bath. The other pair was maintained at −10 °C in a freezer for 20 min. Afterward, the tubes were centrifuged at 1300 × g for 3 min and the haemoglobin content of the supernatant was estimated using Spectronic 21D (Milton Roy) Spectrophotometer at 540 nm.

The percent inhibition of haemolysis by the extract was calculated as:

$$\%\,\text{Inhibition of Haemolysis} = 1 - \frac{OD2 - OD1}{OD3 - OD1} \times 100,$$

where OD1 = absorbance of the test sample unheated. OD2 = absorbance of the test sample heated. OD3 = absorbance of the control sample heated. From the % inhibition, the results are then expressed as IC_{50} value.

Hypotonicity induced haemolysis

Samples of the extract used in this test were dissolved in distilled water (hypotonic solution). The hypotonic solution (500 µL) containing graded doses of the extracts (10, 20, 40, 80, and 100 µg/mL) were put into duplicate pairs (per dose) of the centrifuge tubes. Isotonic solution (500 µL) containing graded doses of the extracts (10–100 µg/mL) were also put into duplicate pairs (per dose) of the centrifuge tubes. Control tubes contained 500 µL of the vehicle (distilled water) and 500 µL of 20 µg/mL of diclofenac sodium, respectively. Erythrocyte suspension (10 µL) was added to each of the tubes and mixed gently. The mixtures were incubated for 1 h at room temperature (37 °C), and afterward, centrifuged for 3 min at 1300 × g. Absorbance (OD) of the haemoglobin content of the supernatant was estimated at 540 nm using Spectronic 21D (Milton Roy) spectrophotometer. The percentage heamolysis was calculated by assuming the heamolysis produced in the presence of distilled water as 100%.

The percent inhibition of haemolysis by the extract was calculated thus:

$$\%\,\text{Inhibition of Haemolysis} = 1 - \frac{OD2 - OD1}{OD3 - OD1} \times 100,$$

where OD1 = absorbance of the test sample in an isotonic solution. OD2 = absorbance of the test sample in a hypotonic solution. OD3 = absorbance of the control sample in a hypotonic solution.

Inhibition of albumin denaturation

The reaction mixture of 1% aqueous solution of bovine serum albumin (Sigma) and test extract at different concentration (10–100 µg/mL) was taken in a centrifuge tube and pH was adjusted to 6.8 using 1N HCl. It was incubated at 37 °C for 20 min followed by heating at 57 °C for 20 min. The solution was cooled and absorbance was taken at 660 nm. The results are then expressed as IC_{50} value.

Molecular docking analysis

COX-2 crystal structure (PDB ID: 1PXX) was downloaded from the Protein Data Bank website (http://www.rcsb.org/structure/1PXX) and imported in the molecular docking software Molegro Virtual Docker 6.0 (MVD 6.0). The active site residue Tyr385, Gly526, and Ser530 were set as the search space binding site (X: −21.51, Y: 18.21, Z: −1.82) and these residues were made flexible and soften with a tolerance of 1.0 and strength of 0.90. On the other hand, the 3D geometrically optimised conformer of compounds **4h** and **4c** was imported in the MVD 6.0. The scoring function was set for the Grid Score (MolDock) with 0.30 Å as the grid resolution. Further, the compounds **4h** and **4c** were set for Internal ES (ElectroStatic), Sp^2–Sp^2 torsions and H-bond (Hydrogen bond) evaluation. The docking search algorithm was set for MolDock Simplex Evolution (MSE) for 20 numbers of runs. The MSE parameters were further set for 1200 maximum iterations and population size of 50. Root mean squared deviation, RMSD, threshold was set at 2.00 calculated by auto-morphisms for better accuracy and reliability. The best orientation of compounds **4h** and **4c** was carried forward for the molecular interaction analysis with the COX-2 enzyme.

Binding affinity calculation

Binding affinity was calculated for compounds **4h** and **4c** based on the coefficients of various energy terms (H-bond, E-Intra (vdw), E-Solvation etc) using multiple linear regression (MLR) equations. The MLR equation is further calibrated with a set of more than 200 structurally diverse complexes obtained from the Protein Data Bank with known binding affinities expressed in kJ/mol.

Density functional theory (DFT) study

DFT study was carried out for compounds **4h** and **4c** estimating the band energy gap (HOMO/LUMO gap). The calculation was carried out using the Gaussian (R) 09 System (Gaussian, Inc, USA). The molecular orbital energies including the HOMO and LUMO band gap energies were calculated at DFT/B3LYP level using the 6–31 G basis set with a net charge of zero and a single spin.

Results and discussion

Chemistry

Our initial trial experiments to prepare dihydro-1,3-oxazine **4a** by an MCR protocol involving benzaldehyde (**2a**), ethylamine (**3a**), and β-naphthol (**1**) without using a catalyst or solvent at 100 °C led to unsuccessful results. Refluxing and stirring a mixture of **2a**, **3a**, and β-naphthol using solvents, such as THF, acetonitrile, dichloromethane, ethanol, and methanol, did not give any useful results. But, surprisingly, when the three components were refluxed in ethanol directly with $SiO_2.HClO_4$ for 18 h, the formation of dihydro-1,3-oxazine **4a** was observed (Scheme 1). The reaction mixture was filtered to recover the $SiO_2.HClO_4$. The filtrate was extracted using ethyl acetate and water and dried over anhydrous Na_2SO_4. The pure compound **4a** was isolated by column chromatography (SiO_2). The yield of the solid white product was 90%.

For optimisation, we tested this MCR by varying the reaction conditions and parameters, i.e, the catalytic system, solvent, temperature, refluxing/stirring time, etc. (Table 1). Screening of various solvents with the catalyst was initially evaluated, guided by the template reaction between benzaldehyde, ethylamine, and β-naphthol (Scheme 1).

The shortest time period for the reaction was 18 h in $SiO_2.HClO_4$/ethanol with a 90% product yield being obtained. Thus, ethanol was the most suitable solvent. It was also observed that acetonitrile gave a 90% yield of the product, but the reaction was longer. Using THF, dichloromethane, and methanol also resulted in longer times with lower yields being obtained. We next, examined the quantity of the catalyst (Table 2). Refluxing the reaction mixture in ethanol for 18 h with 4 mol% of $SiO_2.HClO_4$ was found to be optimum; increasing the catalytic amount did not improve the yield.

After optimising the reaction conditions, we next investigated the generality of this reaction for the synthesis of a wide

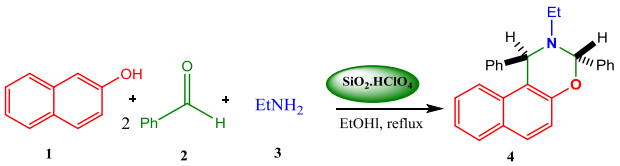

Scheme 1 Synthesis of naphtho[1,2-*e*][1,3]oxazine

Table 1 Optimization of the solvent[a]

Entry	Solvent	Temp (°C)	Time (h)	Yield (%)[b]
1	–	RT	20	–
2	–	100	20	70
3	EtOH	75	18	90
4	MeCN	82	19	90
5	THF	66	19	86
6	CH_2Cl_2	39	19	88
7	MeOH	64	19	87

[a]Reaction conditions: benzaldehyde (**2a**) (2 mmol), $EtNH_2$ (**3a**) (1 mmol), β-naphthol (**1**) (1 mmol), $SiO_2.HClO_4$ (4 mol %), 18 h

[b]Yield of isolated product

Table 2 Optimisation of the catalyst amount[a]

Entry	Catalyst (mol%)	Time (h)	Solvent	Yield (%)[b]
1	4	18	EtOH	90
2	5	18	EtOH	90
3	6	18	EtOH	90
4	7	18	EtOH	90

[a]Reaction: benzaldehyde (2 mmol), ethylamine (1 mmol), and β-naphthol (1 mmol)

[b]$SiO2.HClO_4$ (4 mol%, 18 h, Yield%)

variety of 1,3-oxazine derivatives and the results are summarised in (Table 3). A wide range of structurally varied aldehydes and amines were reacted with β-naphthol to give the corresponding dihydro-1,3-oxazine derivatives in good yields. From Table 3, it can be clearly seen that the reaction required strong ring activating groups such as *p*-OMe, *p*-Me and *o*-Me in order to proceed smoothly to give the desired products. Interestingly, the *p*-MeO substituted benzaldehyde and simple benzaldehyde gave the highest yields. Similarly, when we used ring-deactivating groups, such as $–NO_2$, –F, –Cl-substituted benzaldehydes, moderate yields of the products were obtained. However, except for the *o*-Me substituted benzaldehyde, all the other reactions of substrates with *o*-, *m*- and 2,4-disubstituted electron donating or with withdrawing substituents failed, either giving back the starting materials or inseparable products. In the case of the amines, the reaction proceeded smoothly with primary amines only; bulky amines such as aromatic amines failed to give the corresponding products.

Probable mechanism

The plausible mechanism is shown in Scheme 2, even though we were unable to prove experimentally the formation of the intermediates. The mechanism involves the formation of an imine intermediate with dehydration leading to the final naphtho-fused oxazine. Probably, the role of $SiO_2.HClO_4$ is to activate the benzaldehyde and the intermediates possessing carbonyl functional groups.

Since these oxazines contain two chiral centres, there are possibilities for the formation of the syn- or anti-product. Theoretically, we expected the anti-product rather than the syn product. We thought of confirming the conformations of the structures by single-crystal X-ray studies; however, the literature (Zhang 2009; Yong et al. 2008; Cristina et al. 2001) had already revealed the anti-configuration based on single-crystal structures. The physical properties of the reported compounds were compared with our newly synthesised compounds and their spectral and analytical data were found to be in agreement with our proposed structures. As a representative example, the spectral and analytical data of 2-ethyl-1,3-Bis(4-fluorophenyl)-2,3-dihydro-1*H*-naphtho [1,2-*e*][1,3]oxazine (**4e**) have analysed along with the NOESY and COSY spectra (see the Supporting Information). The proton NMR spectrum showed peaks at 1.01 (t, $J = 8.0$, 3H), 1.30 (q, $J = 9.6$, 2H), 5.40 (s, 1H), 5.60 (s, 1H), 7.01–7.16 (m, 8H), 7.22–7.26 (d, $J = 5.6$, 2H), 7.38–7.34 (d, $J = 9.6$, 2H), 7.59–7.55 (d, $J = 9.6$, 1H), 7.63–7.59 (d, $J = 8.4$, 1H) ppm. The ^{13}C NMR spectrum exhibited signals at 14.4, 21, 39.1, 58.1, 86.2, 113.1, 115.0, 124.2, 126.3, 127.2, 129.0, 131.2, 133.1, 136.1, 137.5, 139.2, 141.0, 153.1, 162 (d, $J_{C\text{-}F} = 43.2$ Hz), 163 (d, $J_{C\text{-}F} = 43.5$ Hz). The structure was further confirmed by the mass spectrum (ESI-MS) with a prominent mass ion peak at *m/z*: 399, calcd. for $C_{26}H_{19}F_2NO$: 402.12 $(M + H)^+$.

The unambiguous structural orientation of the diastereomeric compounds were confirmed from the COSY and NOESY spectra of representative compound **4e**. From the analysis of the COSY spectrum, we found that the protons of the methyl carbon correlate with the protons of the methylene carbon. There were no cross peaks in the chemical shift region for the protons at 2 and 4 (Fig. 3). The absence of cross peaks in this region provided additional information that no coupling occurs between the two chiral protons and thus suggests the anti-conformation of the product. Moreover, the region in the chemical shift range 6.81–7.92 ppm represents the correlations between different aromatic protons. From the NOESY spectrum, no cross peaks were observed and two distinct singlets were present at 5.41 and 5.93 ppm, which is possible with the anti-conformation. Thus, from all these observations and by analogy, we have confirmed that the prepared compounds are anti-1,3-oxazines.

Pharmacological screening

The prepared anti-1,3-oxazine derivatives **4** were then screened against inflammation. Most of the compounds at doses 10–100 µg/mL showed protection of erythrocytes against heat-induced lysis. The IC_{50} value of lysis was different for each compound tested (Table 4). Some compounds showed more protective effects against haemolysis as compared with standard NSAIDs drugs such as diclofenac ($IC_{50} = 30.14$ µg/mL). Oxazines **4a, 4c, 4d, 4h**, and **4n** were more active than the diclofenac standard. Among the tested compounds, **4h** showed the best activity with $IC_{50} =$ 4.807 µg/mL.

The tested compounds (10–100 µg/mL) showed protective effects against isotonic buffer and water-induced lysis. The IC_{50} values of lysis inhibition of the synthesised compounds were higher than that obtained for diclofenac, except oxazine **(4h). 4h** showed the highest activity in the hypotonicity-induced haemolysis assay with lower IC_{50} of 7.37 µg/mL and IC_{50} of 4.807 µg/mL in heat induced haemolysis (Table 4). The albumin denaturation inhibitory

Table 3 Substrate scope for the synthesis of *trans*-1,3-diaryl-1*H*-naphtho[1,2-*e*][1,3]oxazines **4**[a]

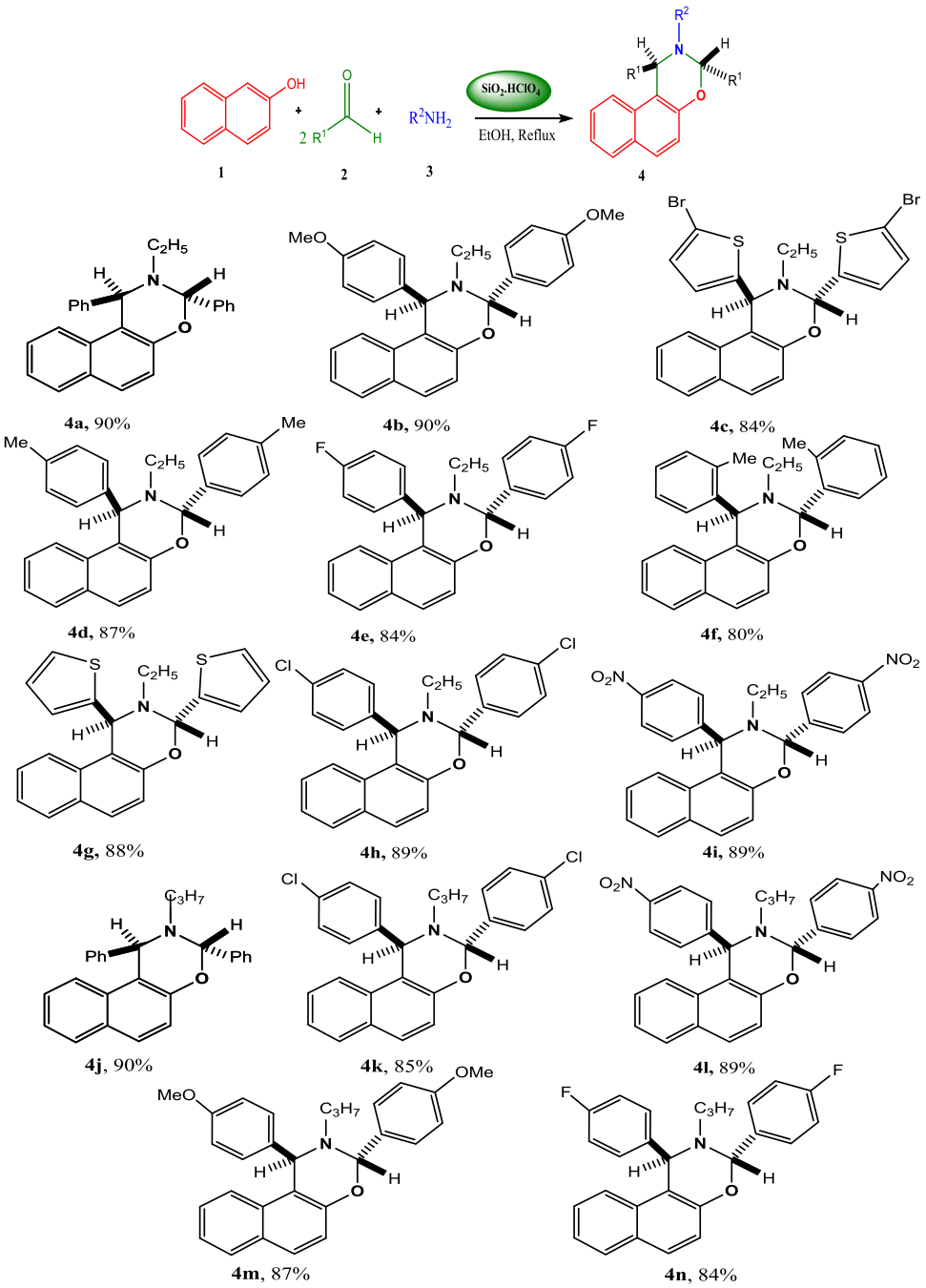

[a]Reaction conditions: aldehyde (2 mmol), amine (1 mmol) and β-naphthol (1 mmol), $SiO_2.HClO_4$ (4 mol%), ethanol (20 mL), (reflux, 18 h), Isolated yield

activity assay results are presented in Table 4. In the albumin denaturation assay, **4c** showed the highest activity with $IC_{50} = 5.5$ µg/mL amongst the synthesised compounds. However, **4c** showed weaker inhibitory activity as compared with NSAIDs diclofenac sodium ($IC_{50} = 2.89$ µg/mL) in preventing albumin denaturation.

There are many ways of assessing the anti-inflammatory activity, and yet there is no report that a particular test is better than the other test. Inflammation is a vascular phenomenon and also involves denaturation of protein. The ability of a substance to inhibit haemolysis and denaturation of protein indicates a good candidate for anti-inflammatory

Scheme 2 Tentative mechanism of naphtho[1,2-*e*][1,3]oxazine synthesis

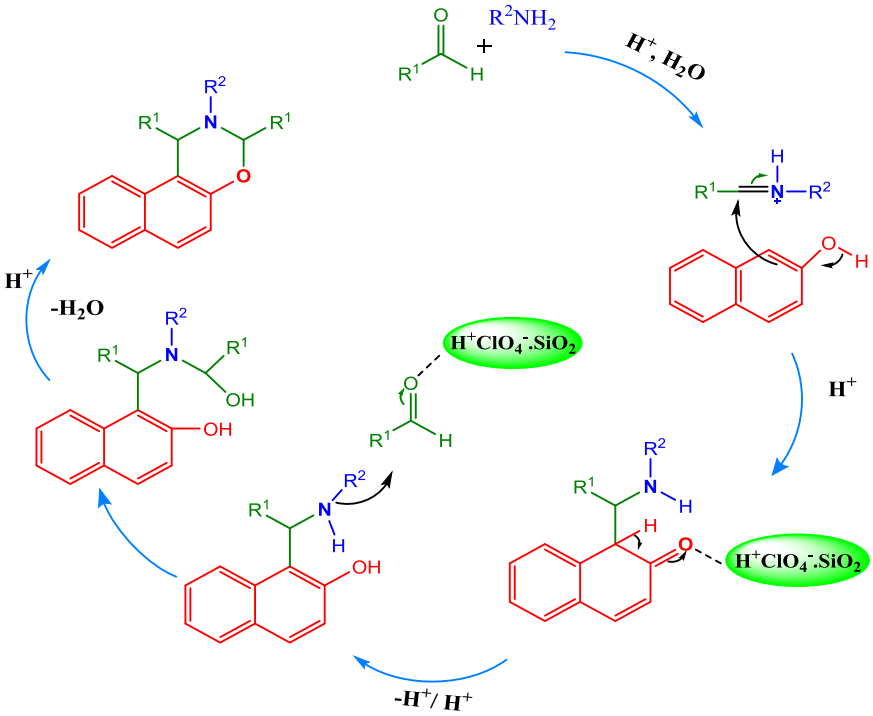

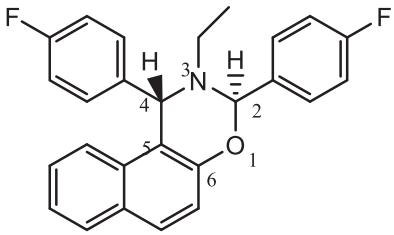

Fig. 3 anti-configuration of 1,3-oxazine, **4e**

agent. Considering this, we have adopted only haemolysis (heat induced and Hypotonicity induced) and albumin denaturation in the present study.

In clinical study, due to their capacity in inhibiting protein denaturation, most of the pharmacological candidate used for the anti-inflammatory and pain-relief management are NSAIDs. **4c** showed the highest activity among all the other compounds in albumin denaturation but weaker than NSAIDs Diclofenac. Though it has IC_{50} comparatively near to that of diclofenac. Compound **4h** is more active in preventing haemolysis but not in albumin denaturation.

Compounds **4c** and **4h** have different physical and chemical properties. **4c** is 1,3-Bis(5-bromothiophen-2-yl)-2-ethyl-2,3-dihydro-1H-naphtho[1,2-*e*][1,3]oxazine having molecular formula $C_{22}H_{17}Br_2NOS_2$ and molecular weight 532.19 g/mol, while **4h** is 1,3-Bis(4-chlorophenyl)-2-ethyl-2,3-dihydro-1H-naphtho [1,2-*e*][1,3]oxazine having molecular formula $C_{26}H_{21}Cl2NO$ and molecular weight 434.36 g/mol. Morphologically **4c** is brown crystalline compound, whereas **4h** is white crystalline compound. Due to the differences in their physico-chemical, morphological, and spatial arrangement, **4c** and **4h** may have different interacting mechanism in inhibiting the denaturation of protein, lysis of RBC membranes and haemolysis. The properties of **4h** might help in preventing the excessive accumulation of fluid within the cell or by preventing the discharge of lysosomal enzymes rendering its highest activity in the haemolytic assay than **4c**.

The synthesised oxazine derivatives at a concentration of 10–100 µg/mL showed protection against lysis induced by heat as well as hypotonic solution. By either preventing the discharge of lysosomal enzymes or by stabilising the lysosomal membranes, NSAIDs showed their beneficial effects as anti-inflammatory agents (Feirrali et al. 1992). The lysis of the membranes, complemented by haemolysis and oxidation of haemoglobin, is caused by contact of RBCs to injurious components, such as hypotonic medium, heat, methyl salicylate, or phenylhydrazine (Kurumbail et al. 1996). Since HRBC membranes are similar to lysosomal membrane components (Halliwell and Whiteman 2004) the inhibition of hypotonicity and heat-induced lysis of RBC membrane was used as a measure of the mechanism of anti-inflammatory activity of the tested principle. The haemolytic effect of the hypotonic solution is associated with excessive accumulation of fluid within the cell, which leads to rupturing of the membrane. RBC membrane injury will render the cell more inclined to secondary destruction through free-radical-promoted lipid peroxidation (Ricciotti and FitzGerald 2011). The pathogenesis of many diseases including arthritis, stroke, and cancer is connected with inflammation (Mizushima 1966).

In order to confirm the anti-inflammatory effects of compounds **4c** and **4h**, molecular docking studies were carried out against the COX-2 enzyme, which is responsible for inflammation and pain. Therefore, targeting the active site of COX-2 followed by inhibiting the enzyme leads to the reduction of pain and inflammation. In this study, the docking scores of compounds **4c** and **4h** docked against the active site of COX-2 are shown in Table 5. Compound **4c** had an overall total score of −252.57 kJ mol^{-1} compared with −198.08 kJ mol^{-1} for compound **4h** and −73.26 kJ mol^{-1} for diclofenac, a known inhibitor of the COX-2 enzyme. Diclofenac is known to inhibit both COX-1 and COX-2. In fact, diclofenac is similar in COX-2 selectivity to celecoxib-a selective COX-2 inhibitor (Gerarldf et al. 2001). Table 6 shows the binding affinities of the investigated compounds. Oxazine **4c** has a binding affinity of −38.53, while that of compound **4h** is −35.81 compared with −29.36 for diclofenac. These results suggest that oxazines **4c** and **4h** are good anti-inflammatory compounds because when it comes to binding affinity, lower the negative score, more stability. Hence more negative value, more binding affinity. Figure 4a, b depicts the steric and hydrophobic interactions of compounds **4c** and **4h** at the active site of COX-2. Compound **4c** showed molecular interactions with Ser353, Tyr385, Ser530, Phe381, Trp387, Met522, Phe518, Val523, Arg513, His90, Leu352, Val349, Arg120, and 527, while compound **4h** showed molecular interactions with Tyr 355, Ser 353, His90, Arg513, Ala527, Pro528, Leu531, Arg120, Val116, Val349, Met522, Phe518, Leu352, and Val523. Thus, the heavy molecular interactions suggest a strong binding affinity. Figure 5 depicts the favoured electrostatic interactions of oxazines **4c** and **4h** in the electronegative (green colour) and electropositive (yellow colour) regions. In addition, Fig. 6 shows the overall energy maps suggesting both the compounds reside in an energy pocket which is favoured with various energy parameters, such as hydrogen bond acceptor and donor-favoured regions, etc. Lastly, Figs. 7 and 8 represent the HOMO and LUMO energies of compounds **4c** and **4h**. The band gap energy of compound **4c** is 0.16767, while that of compound **4h** is 0.16321, which indicates a higher reactivity of compound **4c** (Table 7).

The COX-2 crystal structure (PDB ID: 1PXX) was downloaded from the Protein Data Bank website (http://www.rcsb.org/structure/1PXX) and imported in the

Table 4 Anti-inflammatory activity of 1,3-oxazine derivatives **4a–n** against heat-induced haemolysis, hypotonicity-induced haemolysis, and albumin denaturation[a]

	Heat-induced haemolysis IC_{50} (μg/mL) ± SEM	Hypotonicity-induced haemolysis IC_{50} (μg/mL) ± SEM	Albumin denaturation IC_{50} (μg/mL) ± SEM
Standard (diclofenac sodium)	30.14 ± 0.012	14.12 ± 0.001	2.89 ± 0.001
4a	21.94 ± 0.01	9.70 ± 0.02	760.0 ± 0.67
4b	252.0 ± 0.23	82.43 ± 0.26	19.68 ± 0.01
4c	544.38 ± 0.12	85.38 ± 0.01	**5.55 ± 0.02**
4d	17.56 ± 0.05	107.65 ± 0.07	429.65 ± 0.98
4e	20.28 ± 0.01	1500 ± 0.89	4791 ± 23
4f	217.979	20.272	89.616
4g	56.71 ± 0.1	247.13 ± 0.90	212.13 ± 0.001
4h	**4.807 ± 0.10**	**7.37 ± 0.02**	938.73 ± 0.152
4i	27.08 ± 0.01	93.20 ± 1.2	20.29 ± 0.01
4j	46.349	12.19	27.899
4k	45.932	35.809	394.395
4l	28.511	341.719	60.787
4m	32.233	21.646	34.414
4n	23.828	36.202	32.851

[a]Reaction mixture of a 1% aqueous solution of bovine serum albumin (Sigma) and oxazine extract at different concentration (10–100 μg/mL) was taken in a centrifuge tube and the pH was adjusted to 6.8 using 1 N HCl. The mixture was incubated at 37 °C for 20 min followed by heating at 57 °C for 20 min. The solution was cooled and the absorbance was recorded at 660 nm. The results are then expressed as IC_{50} values

Bold values indicates the highest activities shown by compounds **4c** and **4h**

Table 5 Docking Scores of the investigated compounds

Compound	Mol Dock Score	Interaction	H bond	LE1	LE3	Docking Score	Total score
4c	−73.19	−66.53	0	−2.61	10.54	−120.7	−252.57
4h	−25.75	−47.4	−1.59	−0.86	12.87	−135.36	−198.08
Diclofenac	11.99	2.74	0.11	0.63	11.43	−100.16	−73.26

Table 6 Binding affinities of the investigated compounds

Compound	E-Intra (steric)	E-Intra (tors)	E-Intra (vdw)	Heavy Atoms	MW	Pose energy	Torsions	Binding affinity
4c	−7.26	0.61	66.60	28.00	535.31	−120.77	3.00	−38.53
4h	20.52	1.13	220.16	30.00	434.36	−135.36	3.00	−35.81
Diclofenac	3.05	6.20	57.29	19.00	294.13	−100.16	3.00	−29.36

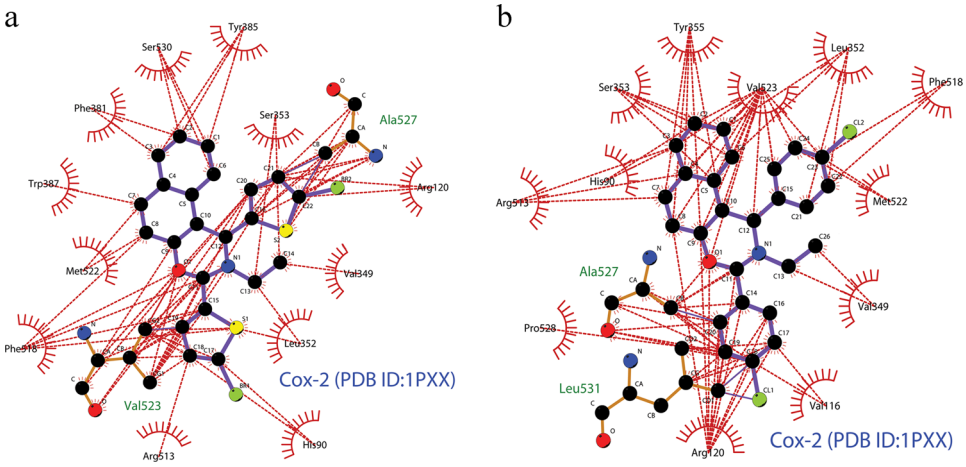

Fig. 4 2D interaction map of compounds **4c** (**a**) and **4h** (**b**) at the active site of the COX-2 enzyme

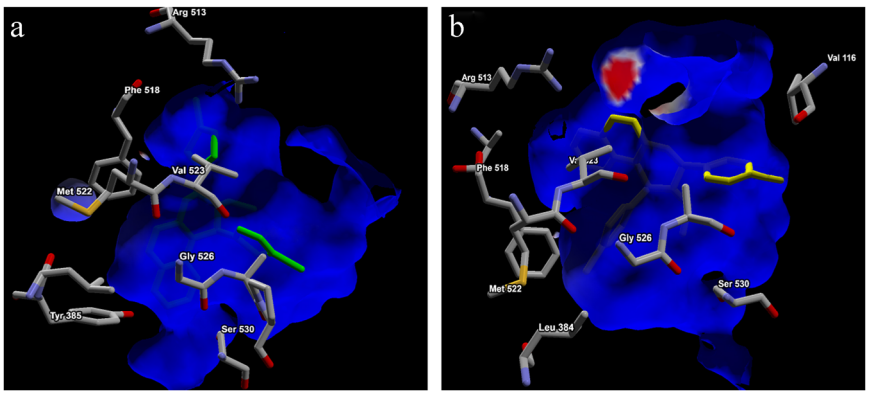

Fig. 5 Electrostatic interactions maps of compounds **4c** (**a**) (green colour) and **4h** (**b**) (yellow colour) at the active site of the COX-2 enzyme

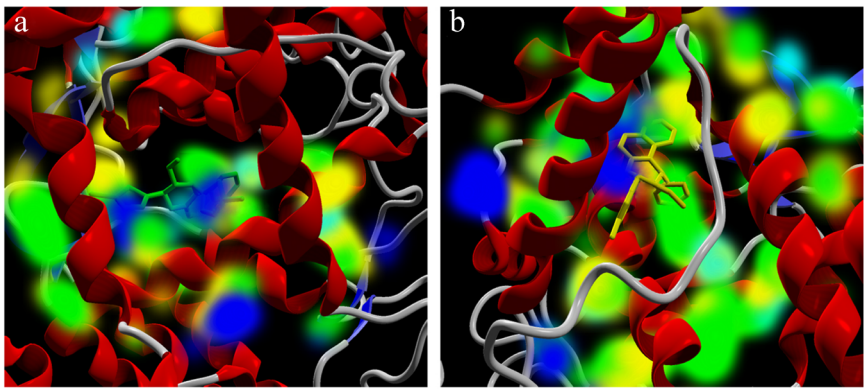

Fig. 6 Energy maps of compounds **4c** (**a**) (green colour) and **4h** (**b**) (yellow colour) at the active site of the COX-2 enzyme

molecular docking software Molegro Virtual Docker 6.0 (MVD 6.0). The active site residues Tyr385, Gly526, and Ser530 were set as the search space binding site (X: −21.51, Y: 18.21, Z: −1.82) and these residues were made flexible and softened with a tolerance of 1.0 and a strength of 0.90. On the other hand, the 3D geometrically optimised conformers of compounds **4c** and **4h** were imported in MVD 6.0. The scoring function was set for the Grid Score (MolDock) with 0.30 Å as the grid resolution. Further, compounds **4c** and **4h** were set for Internal ES (Electro-Static), sp^2–sp^2 torsions and H-bonds (hydrogen bond) evaluation. The docking search algorithm was set for MSE for 20 runs. The MSE parameters were further set for 1200 maximum iterations and population size of 50.

The RMSD threshold was set at 2.00 calculated by automorphisms for better accuracy and reliability. The best orientations of compounds **4c** and **4h** were carried forward for the molecular interaction analysis with the COX-2 enzyme.

Binding affinities were calculated for compounds **4c** and **4h** based on the coefficients of various energy terms (H-bond, E-Intra (vdw), E-solvation etc.) using MLR

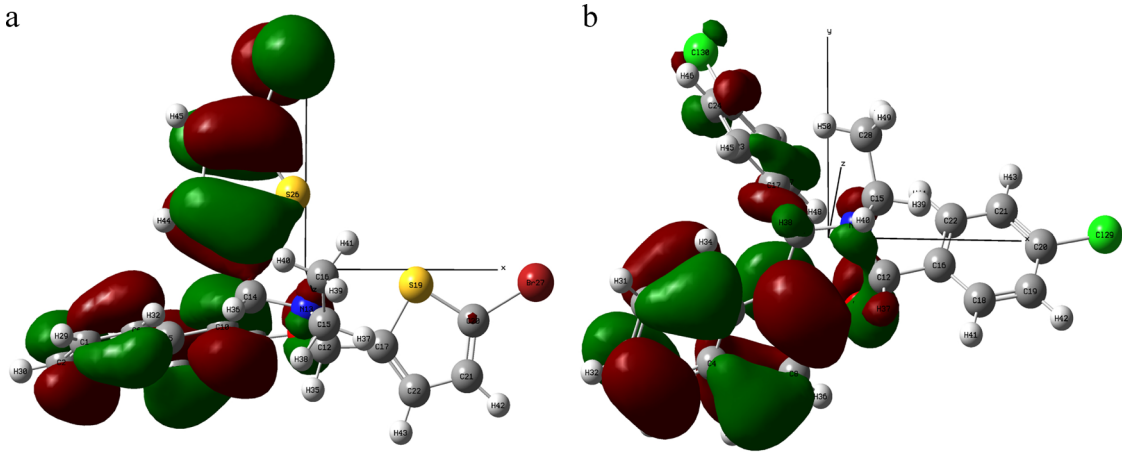

Fig. 7 Molecular orbitals depicting the HOMO energies of compounds **4c** (**a**) and **4h** (**b**)

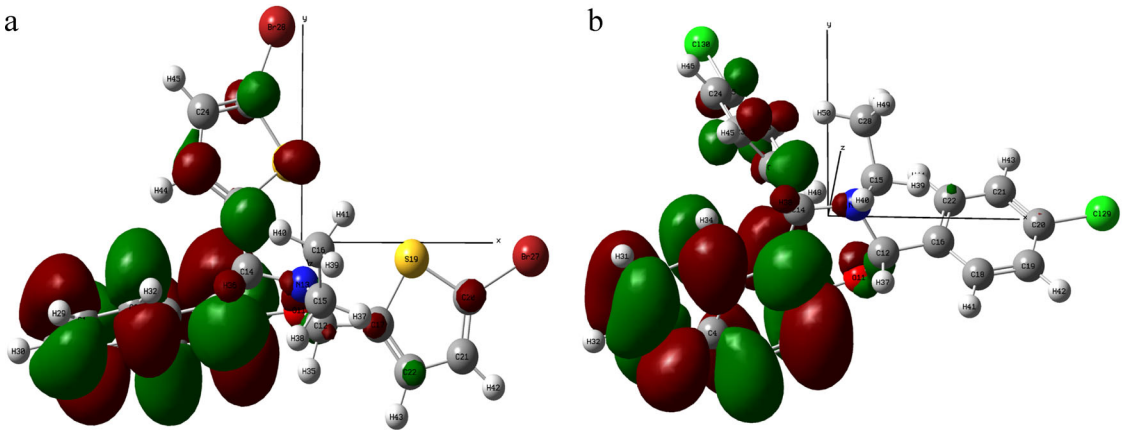

Fig. 8 Molecular orbitals depicting the LUMO energies of compounds **4c** (**a**) and **4h** (**b**)

Table 7 HOMO and LUMO parameters of Compounds **4h** and **4c** optimised at DFT/B3LYP 6-31G basis set

SN	Parameters	Compound (4h)	Compound (4c)	Diclofenac
1	Electronic energy	−6918.32 Hartree	−2053.82 Hartree	−1665.74 Hartree
2	Dipole moment	4.69 Debye	3.62 Debye	4.87 Debye
3	Polarizability	312.47 a.u.	306.47 a.u	238. 41 a.u
4	Nuclear repulsion energy	3912.32 Hartree	3055.61 Hartree	1757.18 Hartree
5	Electronic spatial extent	18416.18 a.u.	15813.94 a.u.	5229.94
6	LUMO	−0.04753	−0.04542	−0.00629
7	HOMO	−0.21074	−0.21303	−0.24598
8	Band Gap ($\Delta E = E_{\text{LUMO-HOMO}}$)	**0.16321**	**0.16761**	**0.23969**

Bold values indicates the highest activities shown by compounds **4c** and **4h**

equations. The MLR equation is further calibrated with a set of more than 200 structurally diverse complexes obtained from the Protein Data Bank with known binding affinities expressed in kJ/mol.

The DFT studies were carried out for compounds **4c** and **4h** estimating the band energy gap (HOMO/LUMO). Calculations were carried out using the Gaussian (R) 09 System (Gaussian, Inc, USA). The molecular orbital energies including the HOMO and LUMO band gap energies were calculated the DFT/B3LYP level using the 6–31 G basis set with a net charge of zero and a single spin.

Conclusion

In conclusion, we have synthesised a series of dihydro-1,3-oxazine derivatives using $SiO_2.HClO_4$ as an effective heterogeneous catalyst using β-naphthol, aliphatic amines, and aromatic aldehydes. The anti-inflammatory activities of the prepared compounds were evaluated and observed significant results. The in silico studies revealed that compounds **4c** and **4h** docked at the active site of the COX-2 enzyme with favourable docking scores and binding affinities compared with diclofenac. Further, in vivo testing of the anti-inflammatory activities of compounds **4c** and **4h** as anti-inflammatory agents are under investigation.

Acknowledgements LVC is thankful to DST, New Delhi, for giving financial assistance in the form of an Inspire Fellowship. OMS is grateful to the CSIR for financial assistance (CSIR project No. 02 (0251)/15/ EMR-II). SPS acknowledges the Department of Biotechnology (DBT), Ministry of Science and Technology, Government of India for granting the DBT-Research Associateship (DBT-RA) for the North-East Region.

Compliance with ethical standards

Conflict of interest The authors declare that they have no conflict of interest.

Publisher's note Springer Nature remains neutral with regard to jurisdictional claims in published maps and institutional affiliations.

References

Artis D, Spits H (2015) The biology of innate lymphoid cells. Nature 517:293–301

Benameur L, Bouaziz Z, Nebois P, Bartoli MH, Boitard M, Fillion H (1996) Synthesis of furonaphth[1,3]oxazine and furo[1,3]oxazinoquinoline derivatives as precursors for an o-quinonemethide structure and potential antitumor agents. Chem Pharm Bull 44:605–608

Cocuzza AJ, Chidester DR, Cordova BC, Jeffrey S, Parsons RL, Bacheler LT, Viitanen SE, Trainor GL, Ko SS (2001) Synthesis and evaluation of efavirenz (Sustiva) analogues as HIV-1 reverse transcriptase inhibitors: replacement of the cyclopropylacetylene side chain. Bioorg Med Chem Lett 11:1177

Cristina C, Andrea M, Gianni P, Emanuela V (2001) Solvent-free asymmetric aminoalkylation of electron-rich aromatics compounds: stereoselective synthesis of aminoalkylnaphthols by crystallization-induced asymmetric transformation. J Org Chem 66:4759–4765

Daqing S, Shaofeng R, Guolan D, Manman W (2010) Efficient synthesis of Naphtho[1,2,*e*][1,3]oxazine derivatives via a chemoselective reaction with the aid of low-valent titanium reagent. J Comb Chem 12:25–30

Feirrali M, Signormi C, Ciccolili L, Comporti M (1992) Iron release and membrane damage in erythrocytes exposed to oxidizing agents, phenylhydrazine, divicine and isouramil. Biochem J 285:295–301

Gerarldf et al. (2001) The coxibs, selective inhibitor of Cox-2. N Engl J Med 345(6):433–42

Hawkey CJ (1999) COX-2 inhibitors. Lancet 353:307–314

Halliwell B, Whiteman M (2004) Measuring reactive species and oxidative damage in vivo and in cell culture: how should you do it and what do the results mean? J Pharm 142:231–255

Hsieh PW, Hwang TL, Wu CC, Chang FR, Wang TW, Wu YC (2005) The evaluation of 2,8-disubstituted benzoxazinone derivatives as anti-inflammatory and anti-platelet aggregation agents. Bioorg Med Chem Lett 15:2786

Harish RT, Sibaprasad S, Ashutosh VB (2012) Synthesis of chiral helical 1,3-oxazines. Org Lett 14:3166–3169

Istvan S, Tamas AM, Laszlo L, Andreas K, Erich K, Kari N, Ferenc F (2004) Stereoelectronic effect in ring-chain tautomerism of 1,3-diarylnaphth[1,2-e][1,3]oxazines and 3-Akyl-1-arylnapth[1,2,e][1,3]oxazines. J Org Chem 69:3645–3653

Ji-Yeon K, Mua Y, Xiangdan J, Park SH, Pham VT, Song DK, Lee KY, Ham WH (2011) Efficient and stereoselective syntheses of DAB-1 and d-fagomine via chiral 1,3-oxazine. Tetrahedron 67:9426–9432

Jin T, Kim JS, Mu Y, Park SH, Jin X, Kang JC, Oh CY, Ham WH (2014) Total synthesis of methyl l-daunosaminide hydrochloride via chiral 1,3-oxazine. Tetrahedron 70:2570–2575

Kurumbail RG, Stevens AM, Gierse JK, McDonald JJ, Stegeman RA, Pak JY, Gildehaus D, Miyashiro JM, Penning TD, Seibert K, Isakson PC, Stallings WC (1996) Structural basis for selective inhibition of cyclooxygenase-2 by anti-inflammatory agents Nature 384:644–648

Kurz T (2005) Synthesis of novel pyrido [2, 3-e][1, 3] oxazines. Tetrahedron 61:3091

Kajjout Md, Michael S, Jacques L, Rolando Ch (2013) A new approach to the synthesis of (Z) 2-fluoro-2-alkenals via wittig-type carbonyl condensation reactions of 2-(fluoromethyl)-4,4,6-trimethyl-1,3-oxazine phosphonium bromide. Tetrahedron Lett 54:1658–1660

Lucas SM, Rothwell NJ, Gibson RM (2006) The role of inflammation in CNS injury and disease. J Pharm 147:S232–S240

Lee WC, Shen HC, Hu WP, Lo WS, Murali C, Vandavasi JK, Wanga JJ (2012) Iodine catalysed, stereo- and regioselective synthesis of 4-arylidene-4H-benzo[*d*][1,3]oxazines and their applications for the synthesis of quinazoline 3-oxides. Adv Synth Catal 354:2218–2228

Lanas A, Chan FK (2017) Peptic Ulcer disease. Lancet 5:613–624

Leimajam VC, Thokchom PS, Laishram RD, Okram MS (*2018*) Synthesis bioactive heterocycles using reusable heterogeneous catalyst $HClO_4$–SiO_2 under solvent free conditions. Green Chem Lett Rev 3:352–360

Mizushima Y (1966) Screening test for antirheumatic drugs. Lancet 288:443

Mathew BP, Kumar A, Sharma S, Shukla PK, Nath M (2010) An eco-friendly synthesis and antimicrobial activities of dihydro-2H-benzo- and naphtho-1,3-oxazine derivatives. Eur J Med Chem 45:1502–1507

Maria CM, Liliana R, Orelli (2016) Microwave-assisted synthesis of 2-Aryl-2-oxazolines, 5,6-dihydro-4H-1,3-oxazines and 4,5,6,7-tetrahydro-1,3-oxazepins. Org Lett 18:6116–6119

Okram MS, Joychandra S, Babita MD, Nalini LD, Irabanta NS, Lee SG (2008) Synthesis and in vitro evaluation of the antifungal activities of dihydropyrimidinones. Bioorg Med Chem Lett 18:6462–6467

Puwen Z, Eugene A, Terefenko, Andrew F, Zhimming Z, Yuan Z, Jeffrey C, Richard W, Jay W, Johny Y (2002) Potent nonsteroidal progesterone receptor agonists: synthesis and SAR study of 6-aryl benzoxazines. Bioorg Med Chem Lett 12:787–790

Prasanta S, Bhattacharya S, Okram MS (2013) Indium/TFA-catalysed synthesis of tetracyclic [6,5,5,6] indole ring via a tandem cycloannulation of β-oxodithioester with tryptamine. Org Lett 15:1974–1977

Park SH, Kim JY, Kim JS, Jung C, Song DK, Ham WH (2015) 1,3-Oxazine as a chiral building block used in the total synthesis of

(+)-1-deoxynojirimycin and (2R,5R)-dihydroxymethyl-(3R,4R)-dihydroxypyrrolidine. Tetrahedron: Asymmetry 26:657–661

Rock KL, Lai JJ, Kono H (2011) Innate and adaptive immune responses to cell death. Immunol Rev 243:191–205

Ricciotti E, FitzGerald GA (2011) Prostaglandins and inflammation. Biol 31:986–1000

Ruedi KB, Christina F, Paul N, Michael S, Sterner-Kock A, Kock M, Putney L, Ferrick DA, Hyde DM, Love RB (2008) IL-17 producing γδ T cells are required for a controlled inflammatory response after bleomycin-induced lung. Inj Inflamm 31:167

Ren H, Grady S, Gamenara D, Heinzen H, Moyna P, Croft S, Kendrick H, Yardley V, Moyna G (2001) Design, synthesis, and biological evaluation of a series of simple and novel potential antimalarial compounds. Bioorg Med Chem Lett 11:1851

Riveiro ME, De Kimpe N, Moglioni A, Vazquez R, Monczor F, Shayo C (2010) Coumarins: old compounds with novel promising therapeutic perspectives. Curr Med Chem 17:1325–1338

Trelle S, Reichenbach S, Wandel S, Hildebrand P, Tschannen B, Villiger PM, Egger M, Jüni P (2011) Cardiovascular safety of non- steroidal anti-inflammatory drugs. Br Med J 342:c7086

Thokchom PS, Thokchom JD, Ningthoujam PS, Okram MS (2018) GFP chromophores from L-phenylalanine: synthesis, photophysical and thermal properties. Chem Sel 3:6596–6600

Wang YX, Ishida H (2000) Synthesis and properties of new thermoplastic polymers from substituted 3,4-dihydro-2H-1,3-benzoxazines. Macromolecules 33:2839–2847

Waisman A, Liblau RS, Becher B (2015) Innate and adaptive immune responses in the CNS. Lancet Neurol 14:945–955

Yong HL, Min MZ, Yuan Z (2008) Acta crystallographica Section E structure reports. Acta Cryst E64:o1972

Yan-Fei L, Hong-Jian Z, Zhe-Shan Q (2016) Synthesis and anti-inflammatory activity evaluation of novel 3-alkyl-6-(4H-1,2,4-triazol-4-yl)-3,4-dihydro-2H-benzo[e][1,3]oxazine derivatives. Med Chem Res 25:2280–2288

Zhang P, Terefenko EA, Fensome A, Wrobel J, Winneker R, Zhang Z (2003) Novel 6-aryl 1,4-dihydrobenzo[d]oxazine-2-thiones as potent, selective, and orally active nonsteroidal progesterone receptor agonists. Bioorg Med Chem Lett 13:1313

Zhang L (2009) 2-Benzyl-1,3-diphenyl-2,3-dihydro-1Hnaphtho[1,2-e][1,3]oxazine Acta Cryst E65:o1796